2013

FEA Estimation and Experimental Validation of Solid Rotor and Magnet Eddy Current Loss in Single-sided Axial Flux Permanent Magnet Machines

Xu Yang
University of Nebraska-Lincoln, xu.yang@huskers.unl.edu

Dean Patterson
University of Nebraska-Lincoln, patterson@ieee.org

Jerry Hudgins
University of Nebraska-Lincoln, jhudgins2@unl.edu

Jessica Colton
Boulder Wind Power, jessica.colton@boulderwindpower.com

Energy Conversion Congress and Exposition (ECCE), 2013 IEEE
Year: 2013
Pages: 3202 - 3209, DOI: 10.1109/ECCE.2013.6647120

FEA Estimation and Experimental Validation of Solid Rotor and Magnet Eddy Current Loss in Single-sided Axial Flux Permanent Magnet Machines

Xu Yang, Dean Patterson, Jerry Hudgins
Department of Electrical Engineering
University of Nebraska-Lincoln, Lincoln NE 68503
xu.yang@huskers.unl.edu, patterson@ieee.org, jhudgins2@unl.edu

Jessica Colton
Boulder Wind Power
United States
jessica.colton@boulderwindpower.com

***Abstract*—The rotor and magnet loss in single-sided axial flux permanent magnet machines with non-overlapped windings is studied in this paper. FEA estimations of the loss are carried out using both 2-D and 3-D modeling. The rotor and magnet losses are determined separately for stator slot passing and MMF space harmonics from currents in the stator. The segregation of loss between the solid rotor plate and the magnet is addressed. The eddy current loss reduction by magnet segments is discussed as well. The prototype 24 slot/22 pole single-sided AFPMs, fabricated with both single layer and double layer windings are assembled. Methods of loss segregation are illustrated in order to separate the eddy current loss.**

I. Introduction

Axial flux permanent magnet (AFPM) machines have gained much attention because of their disc shaped structure, which is suitable for traction systems such as in hybrid vehicles, and in wind power generation [1]. Non-overlapped windings (NOW) have also become attractive due to the short end-windings and consequent less copper loss, as well as their fault tolerance and flux weakening ability [2]. However, the rotor eddy current losses, which occur both in a solid rotor and in magnets may increase dramatically, because of stator MMF space harmonics, and stator open slotting which is commonly used with form wound coils.

The estimation of rotor and magnet eddy current loss has been studied recently. Some analytical calculation methods are proposed such as in [3], [4]. Most of the models are two-dimensional with simplifying assumptions. Complex equations are derived based on Maxwell equations. In [5], [6], the rotor losses of a 12-slot 10-pole AFPM were measured and a three layer analytical model was used to interpret the experiment result. In [7], [8] analytical calculation of eddy current loss is compared with finite element modeling. However, since the analytical method is based on simplifying assumptions, which neglect some parameter constraints, the results are always overestimated or underestimated.

A finite element model is preferred because its simulation is based on exact physical geometry, although it is time consuming. 2-D FEA is a common approach. In [9], [10], a simplified 2D FEA model is used to speed up the calculation. The impact of MMF harmonics of various orders on rotor loss is analyzed. It is concluded that single layer windings have more rotor loss due the richer sub harmonics than double layer windings. In [11], 2-D FEA of eddy current loss in magnets and rotor back iron is analyzed. However, the use of a 2-D model leads to approximate result due to the limited radial extension of actual magnets and rotor in AFPM machine [12]. In [13], a hybrid calculation method, termed as the finite-element aided analytical method, is presented to accurately predict the eddy loss in AFPM machines. In [14], a 3-D finite element method that considered harmonics of inverters is used to calculate loss in each part of the motor separately. It is proved that eddy current loss in permanent magnets from concentrated or NOW windings are larger than that from distributed windings.

This paper is to estimate the rotor and magnet loss due to stator slotting and MMF space harmonics of a 24 slot/22 pole single-sided AFPM with single layer windings and double layer windings by 2D and 3D FEA modeling. The segregation of loss between the solid rotor plate and the magnet is addressed. Eddy current loss reduction by magnet segmentation is also discussed. The prototype 24 slot/22 pole single-sided AFPMs [15], fabricated with both single layer and double layer windings are assembled. The machines are tested at no load and loaded conditions. Methods of loss segregation are illustrated in order to separate the eddy current loss. Experimental measurements are compared with FEA simulations.

II. Loss Analysis In Machine

The machine power balance is as [16]:

$$P_m - P_e = P_{f+w} + P_{s,Cu} + P_{s,Fe} + P_{r,Slot} + P_{r,NOW} \quad (1)$$

where P_m is the input mechanical power, P_e is the output electrical power, P_{f+w} is the friction and windage loss, $P_{s,Cu}$ is the stator copper loss, $P_{s,Fe}$ is the stator iron loss, $P_{r,Slot}$ is the eddy current loss (in both the solid rotor iron and magnets) caused by stator slotting(which is calculated and measured with no current in the windings),and $P_{r,NOW}$ is the rotor and magnet eddy current loss due to MMF space harmonics caused by non-overlapped windings. One goal of this paper is to determine separately the losses ($P_{r,Slot}$ and $P_{r,NOW}$). The

eddy current loss due to PWM harmonics is not considered in this paper.

A. Eddy Current Loss due to Stator Slotting $P_{r,Slot}$

There is flux density variation due to stator slot opening, which induces eddy currents in the rotor iron and permanent magnets as well. It can be calculated or measured at no load conditions, i.e. when the input current is zero.

B. Eddy Current Loss due to MMF Space Harmonics $P_{r,NOW}$

The non-overlapped windings exhibit a rich spectrum of space harmonics in the air gap MMF distribution. Thus the rotor loss is caused by different orders of MMF harmonics which are asynchronous with the rotor, inducing current in both rotor iron and magnets. The amplitude of the MMF harmonics can be computed by the star of slots theory [17], [18]. Fig. 1. shows the space harmonic contents of a 24 slot/22 pole stator MMF through Fourier analysis, with both single layer winding and double layer winding. The main space harmonic is the order of 11. As is shown, in the single layer windings there is a large magnitude of sub harmonics, which are harmonics lower than the main harmonic order. It is therefore expected that the rotor and magnet loss in single layer windings will be much higher than for the double layer windings.

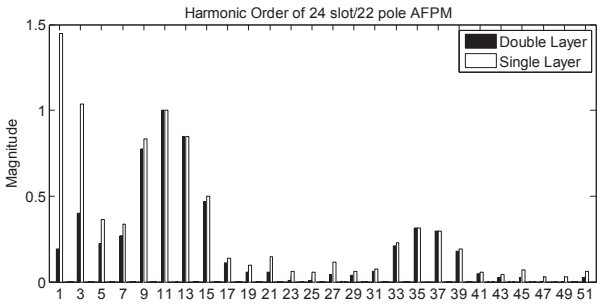

Fig. 1. MMF space harmonic contents of a 24 slot/22 pole AFPM

III. Finite Element Analysis Model of AFPM Machine

The parameters of the 24 slot/22 pole AFPM machine are shown below in Table. I. The stators used for experiments are shown in Fig. 2.(a). The FEA software is Ansoft Maxwell. A 2-D FEA model is generally used to provide a quick calculation. A 3-D FEA model is preferred to evaluate the detailed performances. In the FEA work, and the built machines, each pole is split radially into 2 equal segments, to control eddy current losses in the magnets.

A. 2-D FEA Model

The approach to model the AFPM in 2-D is to view the machine from the side.The geometry is a cylindrical cross-section taken at the average radius as shown in Fig. 2.(b). And rotational motion is assigned to model it as if it was a very small portion of a radial flux machine with a very large radius, for example 100 m, where the center of rotation is vertically above the drawings of Fig. 2. For the 24 slot/22 pole machine,

TABLE I
PARAMETER OF SINGLE-SIDED AFPM

Rated power	6.7 kW
Nominal speed	2800 rpm
Nominal torque	23 Nm
Nominal current	22.5A
Number of slots(Ns)	24
Number of poles(p)	22
Stator outer radius	98mm
Stator inner radius	58mm
Rotor back iron thickness	6mm
Magnet thickness	4mm
Stator steel type	M12-29G
Rotor steel type	mild steel
Magnet type	NdFeB-N40

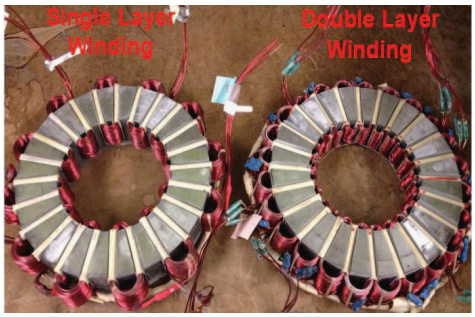

(a) The stators of the 24 slot/22 pole machine

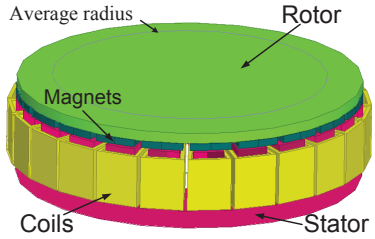

(b) Whole model of the machine

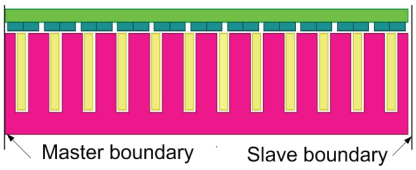

(c) 2-D Modeling

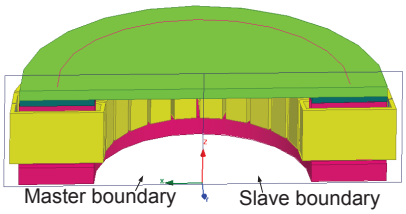

(d) 3-D Modeling

Fig. 2. FEA models

only a very small fraction of the large radial flux machine is modeled. The symmetry multiplier in the FEA is however set to 2 with the master and slave boundary conditions applied. The model is shown in Fig. 2.(c).

B. 3-D FEA Model

The 3-D model is shown in Fig. 2.(d). It is expected that more accurate results will be obtained since the physical

geometry is utilized, though it is time consuming. It is noticed that the torque calculation in FEA remains stable, but the rotor and magnet eddy current loss calculation is sensitive to solver parameters such as mesh, time step and nonlinear solver residual. .

Meshing is critical. Skin effects need to be considered for the eddy current loss calculation. Accordingly to

$$\delta = \sqrt{\frac{2\rho}{2\pi f \mu_0 \mu_r}} \tag{2}$$

in which, δ is the skin depth, ρ is the material resistivity, f is the frequency, μ_r is the relative permeability. The solid steel has skin depth of 0.28 mm at 500 Hz. For the magnet, the NeFeB-N40 has 87 mm at 500 Hz. Thus it needs a fine mesh near the solid rotor plate surface. In order to do that, two layers of skin sheets are created near the surface of rotor plate for meshing. The mesh should not be too coarse or too fine. A good mesh was determined by trial and error. Too fine a mesh leads to unnecessary computation time, and can make the solution unstable

The time step is also crucial. A large time step causes non-physical answers. It was determined that time step should be less than the time of one mechanical degree of rotation. In this simulation, the total number of mesh elements is around 215,205 tetrahedra, in the rotor, there is 143,870 tetrahedra, and the time step at 2800 rpm is 54 us. For a simulation time of 5ms, it takes 10 to 20 hours on an Intel(R) core(TM) i7-2600 CPU3.4 GHz computer with 16G RAM.

C. Eddy Current Loss Calculation in FEA

The algorithm used to calculate the eddy current loss is:

$$P_r = \frac{1}{\sigma} \int_{vol} J^2 \, \mathrm{d}V \tag{3}$$

in which σ is the conductivity of the material, J is the current density,*vol* is the volume. In 2-D FEA, J is the eddy current in the z-direction, P_r is calculated as the integral over the model surface and multiplied by the model depth in the z-direction. In 3-D FEA, it works out element by element the actual current distributions and directions in 3-D space. Thus it should be more accurate.

IV. Simulation Results

A. Eddy Current Loss due to Stator Slotting and MMF Space Harmonics

1) Eddy Current Loss due to Stator Slotting $P_{r,Slot}$: The simulation is first conducted with no current in the stator windings at a range of speeds in order to determine the rotor plate and magnet loss due to stator slotting only. $P_{r,Slot}$ is the same in both single layer and double layer winding since the stator geometries are identical. As shown in Fig. 3, $P_{r,Slot}$ is increased as the speed goes up. However, it can be seen that 2-D FEA and 3-D FEA results differ a lot. Since the 2-D FEA model's current is only in the Z direction, there are no end effects. Thus we expect the loss to be higher in 2-D FEA.

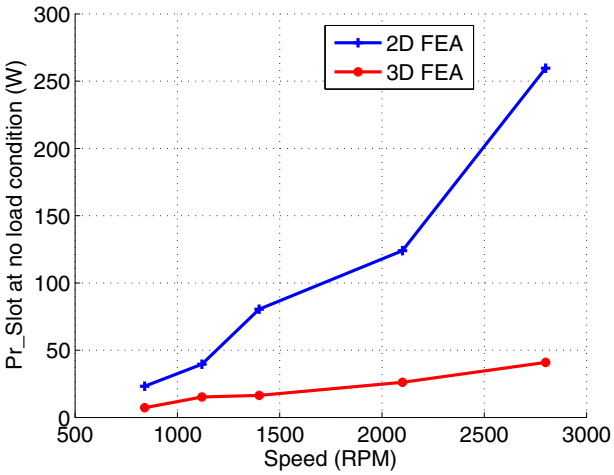

Fig. 3. Eddy current loss $P_{r,Slot}$ due to stator slotting at zero current

2) Eddy Current Loss due to MMF Space Harmonics $P_{r,NOW}$: The same procedure is performed with rated stator current to provide the rated torque for a range of rotor speeds. $P_{r,NOW}$ is separated from the total loss by subtraction of the results of Fig. 3, as shown in Fig. 4. Here it is assumed that $P_{r,NOW}$ remains the same at no load and loaded condition since the flux field does not change much. As can be seen, single layer windings produce more eddy current loss than the double layer windings. With a double layer winding, at 2800 rpm, the eddy current loss due to stator slotting is 41 W, which is slightly higher than $P_{r,NOW}$ which is 37.9 W. With a single layer winding, the major eddy current loss is due to MMF harmonics, at 2800 rpm, which is 113 W and accounts for 73.5% of total loss.

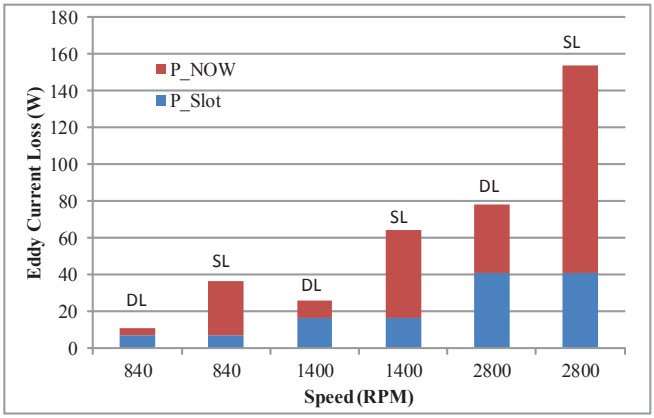

Fig. 4. Eddy current loss $P_{r,NOW}$ due to MMF space harmonics at rated current and various speeds

3) Comments on 2-D FEA and 3-D FEA: It could be seen that 2-D and 3-D FEA results differ a lot. The 3-D FEA should perform more accurately since it models the actual geometry. The simulation time takes about 10 to 20 hours. In contrast, 2-D FEA takes less time, about 10 mins, however, the value of the 2-D results for application to a 3-D machine is in doubt.

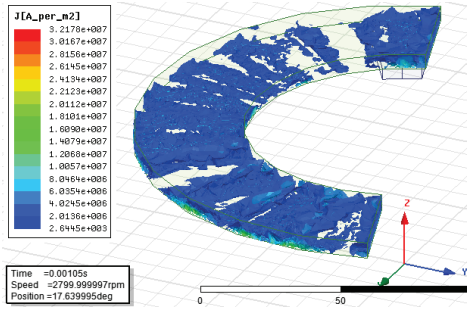

Fig. 5. (a) Eddy current in solid rotor plate

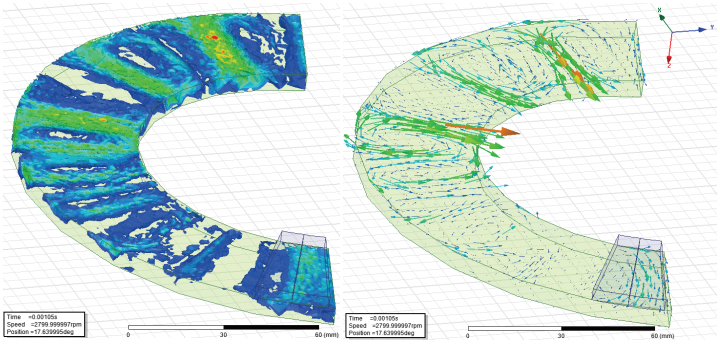

(b) Eddy current in solid rotor plate (view from flipping over)

B. Eddy Current Loss Separation in Solid Rotor Plate and in Magnets

In axial flux machines, a solid rotor plate is used because of mechanical integrity concerns. With a traditional distributed winding, a solid rotor back iron does not experience a strong changing flux field as does the stator steel. However in non-overlapped windings(NOW), the large magnitude of stator MMF harmonics rotating asynchronously with the rotor will induce more eddy current loss in a solid rotor plate.

A 3-D FEA model is implemented. To reduce the simulation time, the center of the rotor plate is subtracted. The eddy current distribution in the solid rotor plate is shown in Fig. 5(a). The current concentrates on the rotor lower surface due to skin effect. Fig. 5(b) provides a better view of the eddy current density and directions by flipping over the rotor plate.

Fig. 6 shows the eddy current loss separation results at rated current in single layer windings by 3 simulations. The total loss is about 154.6 W. The loss in the magnets only of 45.7 W, found by disabling eddy effects in the rotor plate, and the loss in rotor plate only, found similarly of about 114.2 W. The sum of the separated losses is slightly higher than the loss 154.6 W when eddy effects are enabled in both since eddy current in one object actually reduce the flux variations, and hence eddy current losses, in all adjacent conducting objects.

In Fig. 6, it could be seen that the in single layer windings, the eddy current loss in rotor plate is a larger portion of the total loss, compared to double layer winding, due to high MMF sub harmonics.

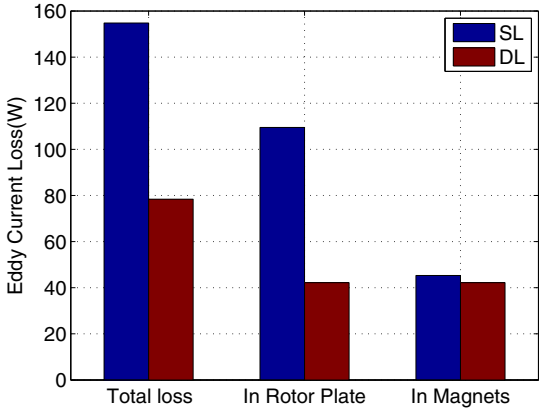

Fig. 6. Eddy current loss separation in single layer winding and double layer winding at rated current and rated speed

1) Eddy Current Loss on Speed Changes: In Fig. 7, it shows the eddy current loss in solid rotor plate and magnets increases linearly on speeds.

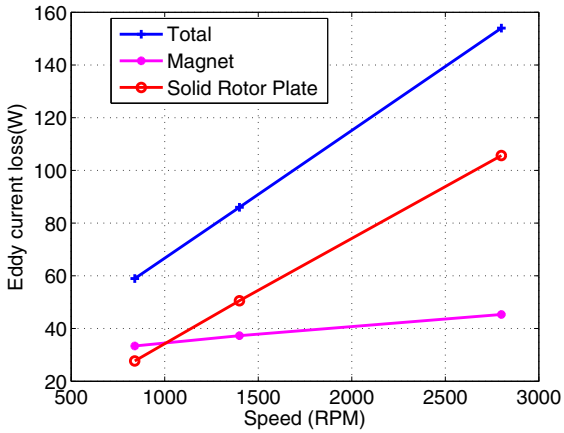

Fig. 7. Eddy current loss in single layer windings at rated current

2) Eddy Current Loss on Current Changes: In Fig. 8, it shows the eddy current loss in rotor plate increases significantly with current increase than in magnets.

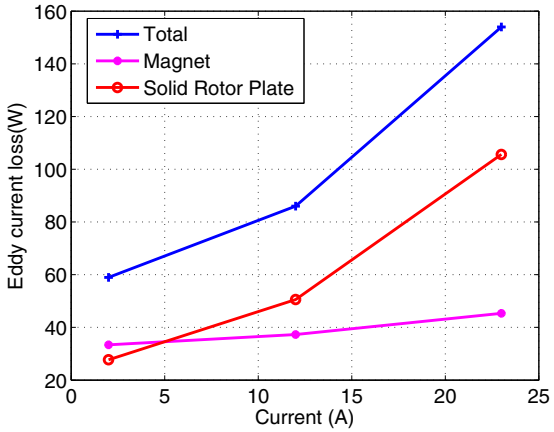

Fig. 8. Eddy current loss in single layer windings at rated speed

Similar results could be obtained in double layer winding machine, the results are not shown here due to space limits.

C. Eddy Current Loss Reduction in the Split Magnets

In FEA and built machines, each pole is split radially into 2 equal segments, to control eddy current losses in the magnets. The eddy current density reduces in the split

magnets, compared with non-split magnets. The simulation results shows that the eddy current loss in split magnets in single layer winding at rated current is 45.7 W , compared to non-split magnets with 85 W eddy current loss, in splitting results in a loss with a reduction of 47 %.

V. Experiment Validation

A. Assembling of the Single-sided AFPMs

The parts of the tested single-side AFPMs including the stators of single layer winding and double layer winding, stator back plate, rotor and rotor back plate. There are two concerns when assembling them together: the axial attractive force and air gap maintenance. The attractive magnetic force between the stator and rotor imposes a high axial load, which is needed to be considered in the bearing selections. Improper selection will cause bearing failures. A proper single row angular contact bearing, which in the stator back plate, is selected to taking the axial load and a single row deep groove ball bearing, which is in the rotor back plate, is chosen to stabilize and position the rotor and shaft to maintain an equal air gap all the way around the stator and prevent wobbling. The bearings are unsealed and with grease to eliminate the friction loss. Shims are used to maintain the air gap. The designed airgap is 1 mm. However in practical experiment, the airgap is set to 1.78 mm. An equipment is designed to introduce the rotor plate to the stator gradually and evenly.

The assembled two machines are shown in Fig.9.:

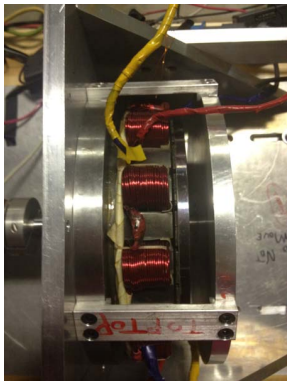

(a) Single layer winding AFPM

(b) Double layer winding AFPM

Fig. 9. Single-sided AFPM machines for experiment

B. Machine Parameters

1) Back EMF Constant: The designed peak value of phase voltage (line to neutral) at rated speed of 2800 rpm is 143 V. The line to neutral voltage waveform of double layer winding machine at 75% rated speed is shown as in the figure. The voltage probe 100mV equals to 50V, thus the peak voltage value of 216 mV is 108 V, which matches the calculated value of 107.25 V. The single layer winding one is not shown here due to space limits.

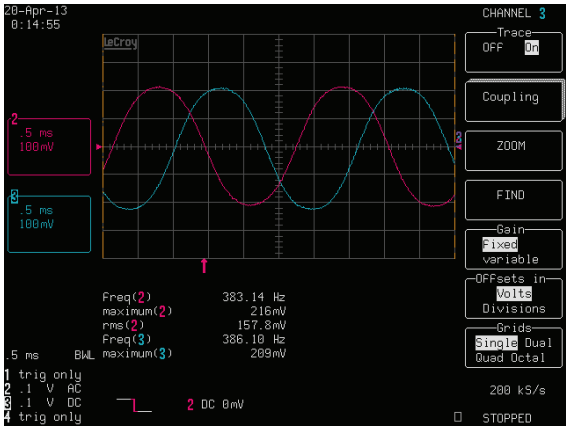

Fig. 10. Line to neutral back EMF of double layer winding AFPM

C. Test Setup

The experiment test setup is shown as in Fig.11.

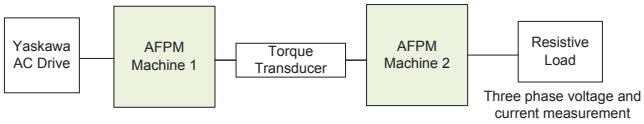

Fig. 11. Test setup

1) AC Drive: The 10 HP Yaskawa drive V1000 is to drive one of the machine as prime mover. Its frequency limit is 400 Hz, which means that it can only achieve 78% of rated speed (513 Hz) of the designed machine.

2) Torque Transducers: For no load test, a lower rating with 2 Nm is used for better accuracy. For loaded test, a large rating with 20Nm is used. NI data acquisition DAQ 9191 is used to obtain the output voltage information from the torque transducer.

3) Resistive Load: The resistive load used is a variable 3.3 kW load, maximum current is 8A at Delta connections. However, in order to reach the rated output power of 6.7 kW, a larger load may be used later.

4) Voltage and Current Measurements: Due to the lab limitations, three line to line voltages are measured by the multimeters and three phase currents are measured by the LeCory current probes.

D. Loss Analysis of the AFPM machines in Tests

The machine power balance, similar to (1) is as:

$$P_m - P_e = P_{f+w} + P_{s,Cu} + P_{s,Fe} + P_{r,Total} \quad (4)$$

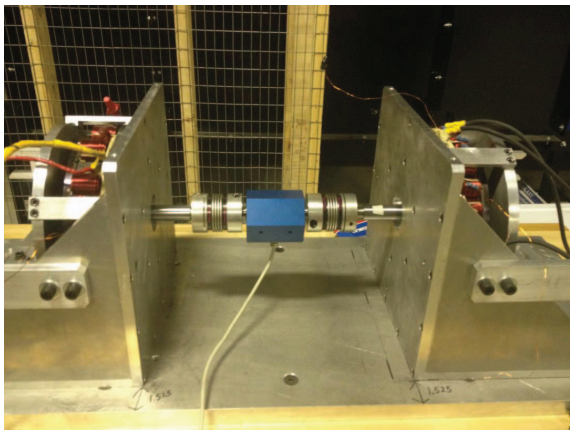

(a) Machine setup

(b) Yaskawa AC drive

(c) 3.3 kW variable resistive load

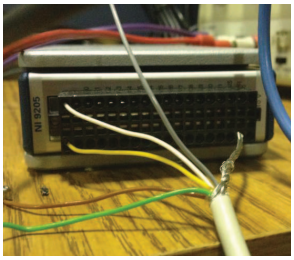

(d) NI DAQ

(e) Torque transducers

Fig. 12. Equipments for the experiment

where $P_{r,Total}$ is the total eddy current loss in both the solid rotor plate and magnets.

P_m is calculated by the measured mechanical torque and speed, P_e is calculated by measuring three phase voltages and currents, P_{f+w} is measured by the test when the stator is replaced with an uncut toroid to isolate the mechanical loss. $P_{s,Cu}$ is calculated by the resistance and currents, $P_{s,Fe}$ is estimated through stator core loss measurement. Thus the eddy current loss $P_{r,Total}$ could be isolated from the measured overall loss which equals to $P_m - P_e$. It should be noted that in the experiment, the eddy current loss in solid rotor plate only and in permanent magnets only are not able be separated.

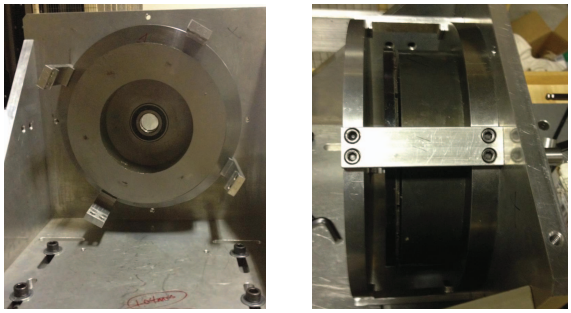

Fig. 13. 'Machine' with a uncut stator

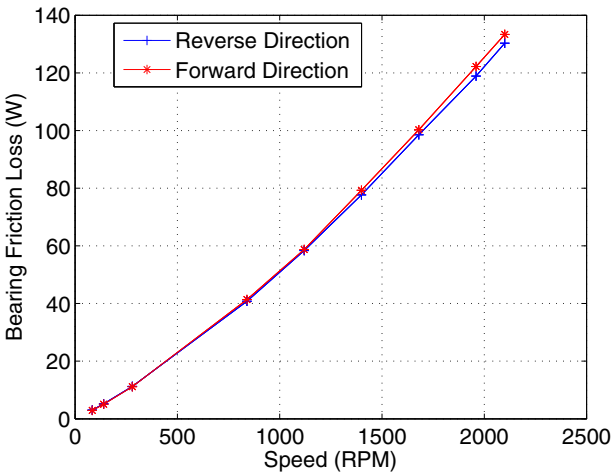

Fig. 14. Bearing and windage loss P_{f+w} results

E. Tests

1) Test 1 Isolate the bearing friction and windage loss: In order to isolate the bearing and windage loss, the stator is replaced by a uncut toroid, which has the same overall dimensions as the wound and slotted stator. The 'machine' is assembled in the same way as previously. For the purpose of ensuring the bearing friction loss in the 'machine' is the same as the bearing friction loss in the actual machine, the axial force between the uncut toroid and the rotor plate should be the same as the one between the actual stator,which has windings in it, and the rotor plate. Through FEA simulation, the air gap needs to be increased to 2.25 mm by adding more shims for equivalent axial force. By magnetostatic solver, the axial force is 1428 newton. Thus, the measured input mechanical power into this 'machine' will be entirely the bearing and windage loss.

The measured loss is taken at both forward (counter clockwise) direction and reverse (clockwise) direction. The bearing loss at various speed from 3% to 75% rated speed are shown as:

2) Test 2 Isolate the stator core loss: The stator core loss is calculated by:

$$P_{s,Fe} = SpecificCoreLossInTeethOnly(f, B_{teeth}) * W_{teeth} + SpecificCoreLossInBackIronOnly(f, B_{backiron}) * W_{backiron}$$

in which, W_{teeth}, $W_{backiron}$ is the weight of teeth and stator back iron

The specific core loss data is measured by the methods in [19]. The specific core loss in teeth are remeasured at different conditions when only one tooth is excited, four teeth are excited and twelve teeth are excited, in order to ensure correctness of the methods and to obtain the most accurate core loss. The flux density in the tooth B_{teeth} is measured by the sensing coil around one tooth in the machine as shown. The flux density in the back iron is accessed by the ratio of $B_{backiron}/B_{teeth}$, which is 0.7 according to 3D FEA.

Fig. 15. Sensing coil in the stator

3) Test 3 No load tests: The rotor and magnet loss due to stator slotting is measured through no load tests.

$$P_{Loss,Noload} = P_{f+w} + P_{s,Fe,noload} + P_{r,Slot} \quad (5)$$

$P_{s,Fe,noload}$ is calculated as in Test 2. The flux density in the teeth is measured through the sense coil voltage as shown in Fig.16. It shows that the flux density in the teeth almost keeps constant, around 1.05 T. Thus, $P_{r,Slot}$ could be separated.

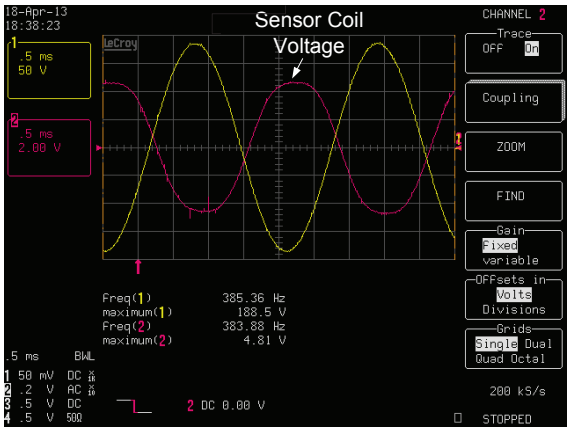

Fig. 16. Sensing coil voltage at no load condition

The no load loss in single layer(SL) winding and double layer(DL) winding machine should be the same since there are no currents. The test results are shown in Fig.17 in both machines and in both forward and reverse directions. It shows they are close.

4) Test 4 Load test: Load tests are performed at different speed from 40%,50%,60%,70%,75% rated speed. At loaded condition, the total loss measured of the machine is:

$$P_{Loss,Loaded} = P_{f+w} + P_{s,Cu} + P_{s,Fe,load} + P_{r,Total} \quad (6)$$

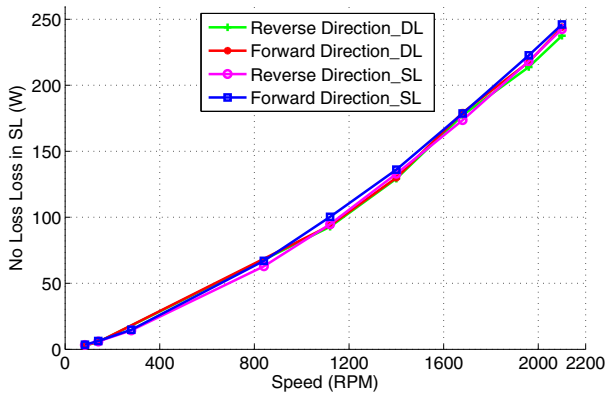

Fig. 17. No load total loss $P_{Loss,Noload}$

The tests are performed firstly at 2A rms phase current. The total loss of single layer winding and double layer winding at 2A loaded current is shown in Fig.18.

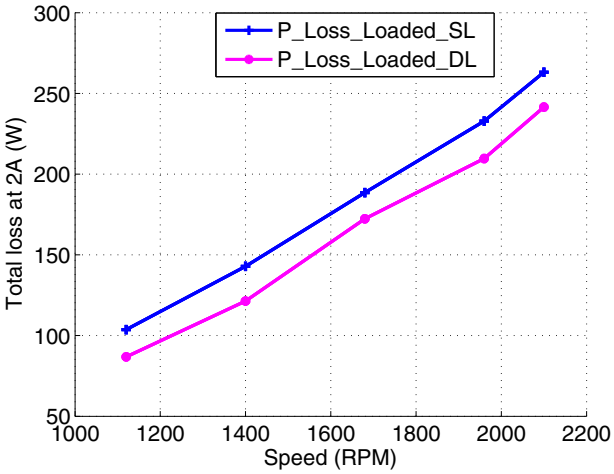

Fig. 18. Load test total loss $P_{Loss,Loaded}$ at 2A rms

The total rotor eddy current loss $P_{r,Total}$ could be obtained by the loss segregation approach described previously.

Due to resistive load limitations, the rated current condition may not be reached at this time.

F. Comparison of the eddy current loss experiment results and FEA simulation results

The separated eddy current loss in experiments is compared with FEA simulations.

1) Eddy current loss at no load condition: Results of eddy current loss due to stator slotting Pr_{Slot} at 30%,40%,50%,75% rated speed, are compared as in Fig.19.

2) Eddy current loss at loaded condition: Results of eddy current loss ($P_{r,Total}$) at 30%,40%,50%,75% rated speed at 2A rms current in single layer windings, are compared as in Fig. 20.

The differences between 3D FEA and experiment results may due to several reasons, the accuracy of each loss parts, especially the estimation of stator core loss. Test results with other loaded currents will be present in the future work to confirm this comparison.

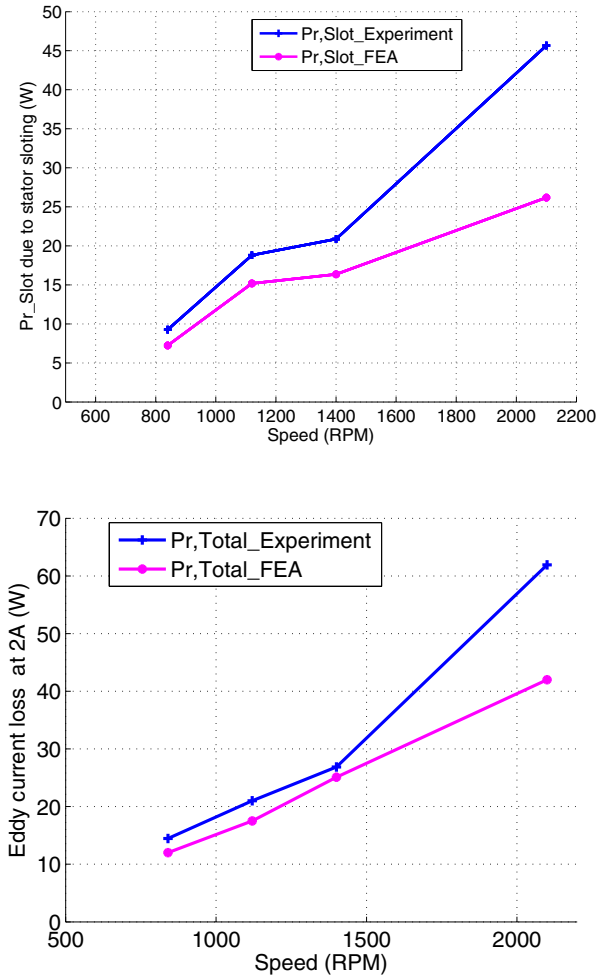

Fig. 20. Eddy current loss at current 2A rms in SL

VI. Conclusion and Future Work

A detailed 2-D and 3-D model process for a 24 slot/22 pole AFPM machine is established. 2-D and 3-D simulation results of eddy current losses due to stator slotting are compared. The segregation of loss between the solid rotor plate and the magnet is addressed. It shows at rated condition in single layer winding, the eddy current loss is mainly due to MMF space harmonics, and mostly in the solid rotor plate rather than in the magnets. In double layer winding, the eddy current loss due to stator slotting and due to MMF space harmonics are close and the loss in the solid rotor plate and in magnet are almost equal.

The built machines are assembled and tested. Methods of loss segregation are illustrated. Experiment measurements show that eddy current loss in single layer winding are higher than in double layer winding. 3D FEA results are compared with experiments results. Test results with other loaded currents will be present in the future work.

References

[1] T.-S. Kwon, S.-K. Sul, L. Alberti, and N. Bianchi, "Design and control of an axial-flux machine for a wide flux-weakening operation region," *Industry Applications, IEEE Transactions on*, vol. 45, no. 4, pp. 1258 –1266, July-Aug. 2009.

[2] A. EL-Refaie, "Fractional-slot concentrated-windings synchronous permanent magnet machines: Opportunities and challenges," *Industrial Electronics, IEEE Transactions on*, vol. 57, no. 1, pp. 107 –121, Jan. 2010.

[3] H. Polinder, M. Hoeijmakers, and M. Scuotto, "Eddy-current losses in the solid back-iron of pm machines for different concentrated fractional pitch windings," in *Electric Machines Drives Conference, 2007. IEMDC '07. IEEE International*, vol. 1, May 2007, pp. 652 –657.

[4] S.-H. Han, T. Jahns, and Z. Zhu, "Analysis of rotor core eddy-current losses in interior permanent-magnet synchronous machines," *Industry Applications, IEEE Transactions on*, vol. 46, no. 1, pp. 196 –205, Jan.-Feb. 2010.

[5] L. Alberti, E. Fornasiero, N. Bianchi, and S. Bolognani, "Impact of rotor losses in a 12-slot 10-pole axial flux pm machine," in *Industry Applications Society Annual Meeting, 2008. IAS '08. IEEE*, Oct. 2008, pp. 1 –8.

[6] L. Alberti, E. Fornasiero, N. Bianchi, and S. Bolognani, "Rotor losses measurements in an axial flux permanent magnet machine," Energy Conversion, IEEE Transactions on,vol. 26, no. 2, June 2011, pp. 639 –645.

[7] A. Jassal, H. Polinder, D. Lahaye, and J. Ferreira, "Comparison of analytical and finite element calculation of eddy-current losses in pm machines," in *Electrical Machines (ICEM), 2010 XIX International Conference on*, Sept. 2010, pp. 1 –7.

[8] D. Ishak, Z. Zhu, and D. Howe, "Eddy-current loss in the rotor magnets of permanent-magnet brushless machines having a fractional number of slots per pole," *Magnetics, IEEE Transactions on*, vol. 41, no. 9, pp. 2462 – 2469, Sept. 2005.

[9] N. Bianchi and E. Fornasiero, "Impact of mmf space harmonic on rotor losses in fractional-slot permanent-magnet machines," *Energy Conversion, IEEE Transactions on*, vol. 24, no. 2, pp. 323 –328, June 2009.

[10] N. Bianchi, S. Bolognani, and E. Fornasiero, "An overview of rotor losses determination in three-phase fractional-slot pm machines," *Industry Applications, IEEE Transactions on*, vol. 46, no. 6, pp. 2338 –2345, Nov.-Dec. 2010.

[11] G. Ugalde, Z. Zhu, J. Poza, and A. Gonzalez, "Analysis of rotor eddy current loss in fractional slot permanent magnet machine with solid rotor back-iron," in *Electrical Machines (ICEM), 2010 XIX International Conference on*, Sept. 2010, pp. 1 –6.

[12] F. Caricchi, F. Maradei, G. De Donato, and F. Capponi, "Axial-flux permanent-magnet generator for induction heating gensets," *Industrial Electronics, IEEE Transactions on*, vol. 57, no. 1, pp. 128 –137, Jan. 2010.

[13] R.J. Wang and M. Kamper, "Calculation of eddy current loss in axial field permanent-magnet machine with coreless stator," *Energy Conversion, IEEE Transactions on*, vol. 19, no. 3, pp. 532 – 538, Sept. 2004.

[14] K. Yamazaki, Y. Fukushima, and M. Sato, "Loss analysis of permanent-magnet motors with concentrated windings-variation of magnet eddy-current loss due to stator and rotor shapes," *Industry Applications, IEEE Transactions on*, vol. 45, no. 4, pp. 1334 –1342, July-Aug. 2009.

[15] J. Colton, "Design of an integrated starter-alternator for a series hybrid electric vehicle: A case study in axial flux permanent magnet machine design," Ph.D. dissertation, University of Nebraska Lincoln, Lincoln, NE, 2010.

[16] J. Colton, D. Patterson, and J. Hudgins, "Rotor losses in axial-flux permanent-magnet machines with non-overlapped windings," in *Power Electronics, Machines and Drives (PEMD 2010), 5th IET International Conference on*, April 2010, pp. 1 –6.

[17] N. Bianchi, S. Bolognani, M. Pre, and G. Grezzani, "Design considerations for fractional-slot winding configurations of synchronous machines," *Industry Applications, IEEE Transactions on*, vol. 42, no. 4, pp. 997 –1006, July-Aug. 2006.

[18] N. Bianchi and M. Dai Pre, "Use of the star of slots in designing fractional-slot single-layer synchronous motors," *Electric Power Applications, IEE Proceedings* -, vol. 153, no. 3, pp. 459 – 466, May 2006.

[19] X. Yang, D. Patterson, and J. Hudgins, "Core loss measurement in the actual finished stator of a single-sided axial flux permanent magnet machine," in *Electric Machines Drives Conference, 2013. IEMDC '13.* , May 2013.